Biotechnology Reports 4 (2014) 21–29

Contents lists available at ScienceDirect

Biotechnology Reports

journal homepage: www.elsevier.com/locate/btre

Preparation of functionalized porous nano-γ-Al_2O_3 powders employing colophony extract

Ángela B. Sifontes [a,*], Brenda Gutierrez [a], Andrea Mónaco [a], Andreina Yanez [a], Yraida Díaz [a], Franklin J. Méndez [a], Ligia Llovera [a], Edgar Cañizales [b], Joaquín L. Brito [a]

[a] Centro de Química, Instituto Venezolano de Investigaciones Científicas, Caracas 1020-A, Venezuela
[b] PDVSA, Intevep, Caracas 1020-A, Venezuela

ARTICLE INFO

Article history:
Received 20 March 2014
Received in revised form 26 June 2014
Accepted 7 July 2014
Available online 21 July 2014

Keywords:
Green synthesis
Nanoparticles
Porous ceramic
Colophony/rosin

ABSTRACT

This study reports the synthesis of porous nano alumina employing carboxylato-alumoxanes $[Al(O)_x(OH)_y(O_2CR)_z]_n$ as precursors for controlling the pore size, pore size distribution and porosity of the alumina, using a new process ecofriendly. The carboxylato-alumoxanes was prepared by the reaction of boehmite with carboxylic acids. The boehmite was obtained by the hydrolysis of aluminum alkoxide in an aqueous solution. The colophony extract is employed as a source of carboxylic acids. The materials were characterized, using XRD, TGA, N_2 physical adsorption, SEM, TEM, NMR and FTIR. A mechanism was proposed for the formation of the synthesized structures. TEM measurements confirmed particle size ranged from 5 to 8 nm.

1. Introduction

Aluminas are important industrial chemicals that have found wide application as adsorbents, ceramics, abrasives, and as catalytic materials [1–3]. In particular, the class of aluminum oxides known as "transition aluminas" plays commercially important role in many chemical processes: these solids have been used as catalysts and catalyst supports for the Claus reaction, cracking, hydrocracking and hydrodesulfurization of petroleum, the steam reforming of hydrocarbon feedstocks ranging from natural gas to heavy naphthas to produce hydrogen, the synthesis of ammonia, and the control automobile exhaust emissions [1–3].

The large applications of transition aluminas in catalysis and adsorption processes can be attributed to a combination of favorable textural properties such as: appropriate pore size distributions, usually bimodal; a high surface area; and surface chemical properties that can be either acidic or basic depending on the transition alumina structure and the degree of hydration and hydroxylation of the surface [1–3]. Structurally, all transition aluminas are disordered crystalline phases. Although the oxygen atoms are arranged in regularly ordered close packed arrays, the aluminum atoms adopt different ways of occupying the tetrahedral and octahedral interstices within the oxygen lattice. In general, the variations in the relative placement of aluminum ions in the tetrahedral and octahedral positions leads to different phases that can be distinguished by NMR techniques and by X-ray diffraction [1–3].

Transition aluminas are formed through the thermal dehydration and dehydroxylation of aluminum trihydroxides or aluminum oxyhydroxides. The thermal dehydration of aluminum trihydroxide (gibbsite) can lead to the formation of χ, κ, ρ, η or θ transition aluminas, depending on the heating rate, the dwell temperature and the atmosphere in contact with the solid phase [1–3]. The thermal dehydration of boehmite can afford γ, η, δ, or θ phases, depending on the conditions of dehydration, the particle size and degree of crystallinity of the starting boehmite. Pseudoboehmite, a poorly ordered form of boehmite with a small primary particle size, is often a preferred precursor to transition aluminas, because it typically affords derivatives with relatively high surface areas and pore volumes. Particularly, γ alumina (γ-Al_2O_3) is formed from well ordered boehmite at a temperature over 500 °C, depending on the particle size. Pseudoboehmite can be transformed to η alumina upon dehydration [1–3].

Carboxylate-alumoxanes are prepared from the reaction of boehmite [Al(O)(OH)]n with carboxylic acid (HO_2CR). Although, they are given the general formula, $[Al(O)_x(OH)_y(O_2CR)_z]_n$ where $2x + y + z = 3$ and $R = C_1–C_{14}$ [1], carboxylate-alumoxanes are in fact

* Corresponding author. Tel.: +58 212 5041342; fax: +58 212 5041741.
E-mail addresses: angelasifontes@gmail.com, asifonte@ivic.gob.ve (Á.B. Sifontes).

http://dx.doi.org/10.1016/j.btre.2014.07.001

alumina nanoparticles between 5 and 200 nm in diameter. The surface of the nanoparticle is covered with covalently bound carboxylate groups [4,5]. Some of the simple carboxylic acids which have been used are: acetic acid, methoxyacetic acid, methoxy (ethoxy) acetic acid, methoxy (ethoxy ethoxy) acetic acid, hexanoic acid etc. Some of the carboxylic acids containing other functionalized groups are: 4-hydroxybenzoic acid, 4-aminobenzoic acid, methacrylic acid, hydroxylacetic acid, aminoacetic acid, 6-aminohexanoic acid, lactic acid, L-lysine etc [4].

Carboxylate-alumoxanes have found applications in a variety of interesting fields, such as the following: synthesis of metal doped aluminum oxides, catalyst components, preparation of ceramic membranes, synthesis of hollow alumina spheres, strengthening of porous alumina ceramics, and fabrication of fiber reinforced ceramic matrix composites, fabrication of biocompatible nanocomposites, polymeric nanocomposites, performance improvements of lithium batteries, non-skid and non-flammable coatings and MRI contrast agents [6,7].

In this sense, we have developed a method for the control of the porosity and pore size distribution on the synthesis of γ-alumina: reacting boehmite with a mixture of carboxylic acids from the extract of rosin, to produce carboxylate-alumoxane nanoparticles; drying the carboxylate-alumoxane nanoparticles; and firing the dried nanoparticles at a temperature of 650 °C.

The rosin, main components of the colophony extract, is a mixture of isomeric cyclic carboxylic acids with the general formula $C_{19}H_{29}COOH$ and it is produced by heating fresh liquid oleoresin to vaporize the volatile liquid terpene components [8,9]. Oleoresins are biological materials, that exude from cuts on living pines, products of the living protoplasm and therefore referable to the original products of photosynthesis for their ultimate chemical derivation [8,9].

The rosin or "mixture of organic acids from colophony" is considered an amphipathic material because the compound contains both hydrophilic and hydrophobic parts [10,11]. For this reason, the rosin provides appropriate conditions to form highly dispersed stable colloidal suspensions [12]. These properties make it an interesting product to be used in the synthesis of materials. Fig. 1, shows the molecular structure of the main component of rosin (abietic acid) showing the hydrophobic and hydrophilic portions [10,11].

2. Materials and methods

2.1. Synthesis of carboxylate alumoxane from pine resin

A sample of 2 g of oleoresin of pine (*Pinus caribaea* spp., Fig. 1), in 60 mL of deionized water was submitted to continuous agitation for 8 h at room temperature. The sample was macerated during 24 h, centrifuged and filtered to separate the solid parts of the extract. Finally it was added under continuous agitation, 0.02 moles of aluminium isopropoxide and dilute nitric acid (10 vol%). The obtained suspension was subjected to agitation for 2 h and aged for 6 h. The resulting solid was dried at 80 °C for 12 h and calcinated at 600 °C for 6 h using a heating rate of 5 °C/min. The boehmite used for comparison was prepared by the Yoldas method [13].

2.2. Characterization

Characterization was carried out by X-ray diffraction, using a Siemens D-5005 diffractometer and CuKα radiation in the 2θ range between 5 and 70°, operating at 40 kV and 20 mA. Thermogravimetric analysis (TGA) was performed from room temperature to 750 °C in a Du Pont 990 thermogravimetric analyzer under air flow (100 mL/min) at a heating rate of 10 °C/min. Fourier transform infrared (FT-IR) spectra, of samples prepared before and after calcinations, were recorded with a Nicolet Magna 500 spectrometer in the range of 4000–400 cm^{-1}.

The textural properties of the calcined oxides were characterized by N_2 adsorption porosimetry (Micromeritics, ASAP 2010). The samples were degassed at 300 °C under vacuum. Nitrogen adsorption isotherms were measured at liquid N_2 temperature (77 K), and N_2 pressures ranging from 10^{-6} to 1.0 P/P_0. Surface area was calculated according to Brunauer–Emmett–Teller (BET) method and the pore size distribution was obtained according to the Barret–Joyner–Halenda (BJH) method [14].

The evaluation by transmission electron microscopy (TEM) was performed on a JEOL JEM-2100 microscope with LaB6 filament (accelerating voltage of 200 kV). The samples were prepared by suspending the powders in an ethanol-based liquid and pipetting the suspension onto a carbon/collodion-coated 200 mesh copper grid. ^1H- and ^{13}C-NMR spectra were measured in a Bruker 400-

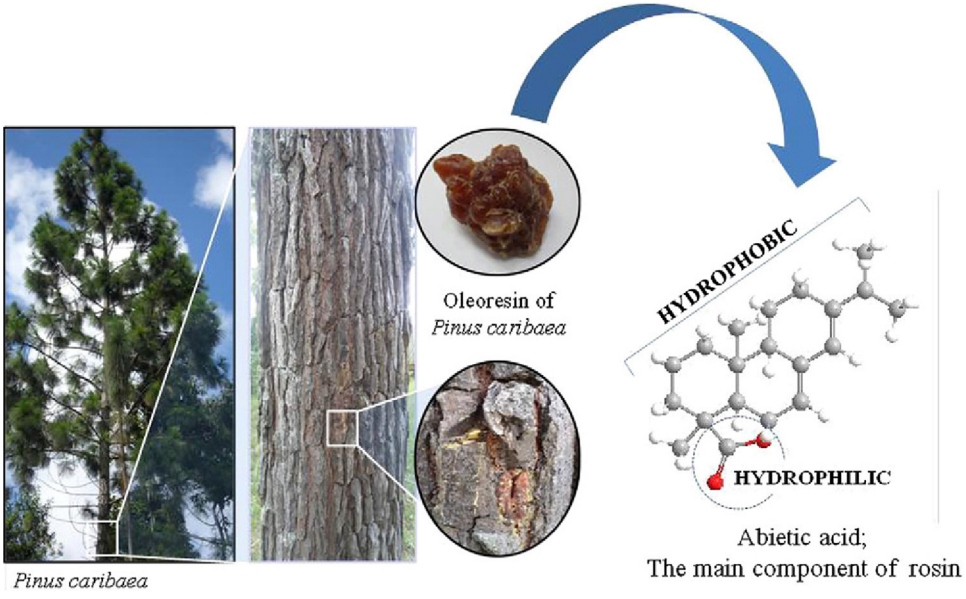

Fig. 1. Oleoresin of *Pinus caribaea* and molecular structure of abietic acid; the main component of rosin.

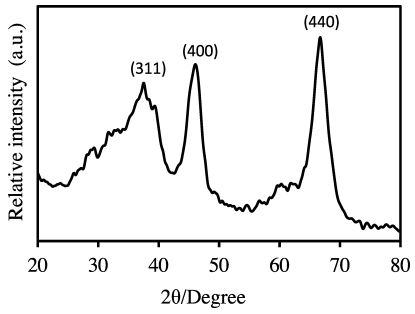

Fig. 2. XRD patterns of synthesized γ-alumina.

Avance spectrometer; in (D6) DMSO; chemical shifts in ppm rel.; dwell time (DW) 48.400 s, acquisition time (AQ) 3.17 s, number of transients (NS) 1024; ^{13}C NMR DW 27.800 s, AQ 1.82 s, NS 60,788. The NMR spectra were calculated for the resinic acids commonly found in the rosin of *Pinus Caribaea* with the ACD/Labs (version software) [15] program.

3. Results and discussion

The crystalline properties of synthesized alumina (γ-Al_2O_3) are shown by the XRD pattern in Fig. 2. The XRD spectra presents three main peaks placed at *d*-spacings of 0.239, 0.197, and 0.140 nm, corresponding respectively to the *d*311, *d*400, *d*440 reflections of γ-Al_2O_3 [11–13]. However, several other metastable aluminum oxides, so-called transition aluminas (such as κ, γ, δ, η and θ) show similar XRD traces, which make phase identification more difficult [3,16].

Fortunately, there are unique values of tetrahedral to octahedral Al ratios that can be utilized for confirming the XRD characteristics of alumina phases [3,16]. For this reason ^{27}Al MAS NMR has been used to observe the structural transformations produced by thermal heating.

The ^{27}Al MAS NMR spectrum of the sample calcined at 650 °C is shown in Fig. 3. In the spectrum two signals at 5.5 and 74.5 ppm were identified, which can be related to the octahedrally coordinated AlO_6 and the tetrahedrally coordinated AlO_4 sites in the alumina matrix, respectively. Penta-coordinated alumina often associated to the presence of amorphous alumina phase is absent. The ratio of tetrahedral to octahedral Al is about 1:3, which is characteristic of γ-Al_2O_3 phase [3,10–18].

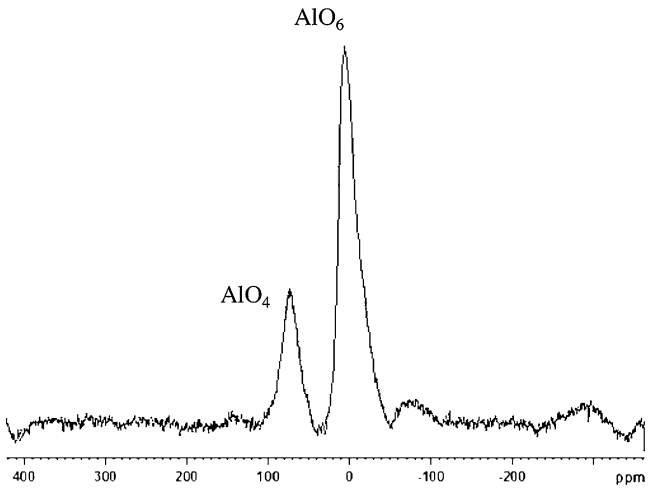

Fig. 3. ^{27}Al MAS NMR spectra of the sample calcined at 650 °C.

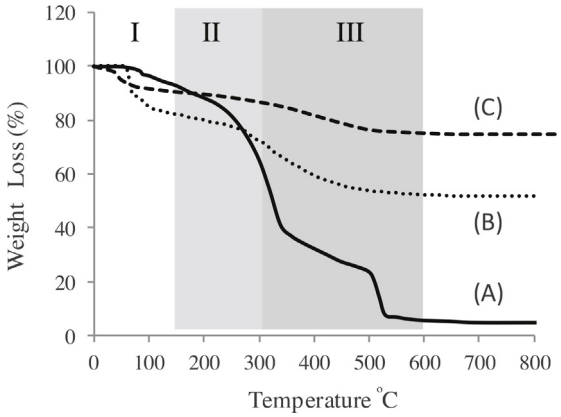

Fig. 4. TG curves of the pure extract (A), as-synthesized sample dried at 80 °C (B) and pure boehmite (C).

Both the XRD patterns and ^{27}Al MAS NMR spectrum seem to indicate that the formation of alumina using metal alkoxide takes place according to the following reaction scheme:

$$Al(OR)_3 + 2H_2O \rightarrow AlOOH + 3ROH$$

$$2AlOOH \overset{600^{\circ}C}{\rightarrow} Al_2O_3 + H_2O$$

It is also important to mention that the thermal dehydration of boehmite (AlOOH) can afford γ, η, δ, or θ phases, depending on the conditions of dehydration, the particle size and degree of crystallinity of the starting boehmite [1,11]. For this reason, it is important to perform a thermogravimetric analysis of the sample to evaluate the dehydration process of boehmite.

Fig. 4(A–C) shows the TG curves of the pine rosin (A), the sample dried at 80 °C (B) and pure boehmite (C), respectively. Boehmite was synthesized in absence of the extract, for purpose of comparison. The TG curve of rosin showed a total weight loss of 93%. A continuous loss up to about 250 °C was followed by a sharp step at this temperature and a second less intense at 530 °C. This could be attributed to the slow elimination of the water in the crystals, and the stepwise pyrolysis of the rosin.

For the boehmite sample, two-step weight loss was observed due to dehydroxylation process. Three steps of weight loss were detected for as-synthesized sample, being thermally stable up to 300 °C, while no changes were evident above 450 °C. The region between 25 °C and 150 °C indicates the desorption of physisorbed water (zone I) [10–12]. Weight loss in the range of temperature 150–300 °C (zone II) could be attributed to the decomposition of organic components [10–12]. The zone III, 300–600 °C was attributed to the loss of water associated with the phase change to form γ-Al_2O_3. However, a fraction of the organic components could be retained by the alumina surface, as will be discussed below. The "plateau" observed above 550 °C in the TG curve indicated that a stable phase had been formed.

The dehydroxylation of boehmite (AlOOH) to γ-Al_2O_3 is known to occur at temperatures higher than 300 °C, and is accompanied by a theoretical weight loss of 15%. The observed weight loss at 300–600 °C (28.16%) for the as-synthesized sample was significantly higher than the theoretical value. This can be attributed to the weight loss by decomposition of the rosin-boehmite complex formed in the synthesis medium, in addition to the dehydroxylation of boehmite to γ-alumina. X-ray diffraction patterns corresponding to the as-synthesized sample and pure boehmite (JCPDS Card 21-1307) are presented in Fig. 5(A and B). The as-synthesized sample dried at 80 °C showed some broad and weak

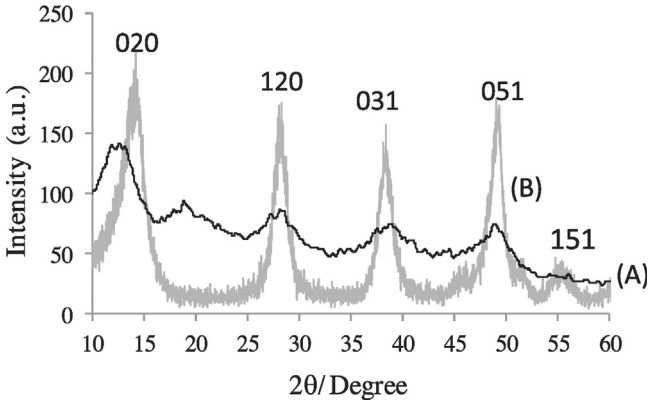

Fig. 5. XRD patterns of as-synthesized sample dried at 80 °C (A) and pure boehmite (B).

peaks in positions that confirm the presence of the boehmite phase, prior to the formation of the γ-phase.

Typical TEM images of the products after calcination at 650 °C are shown in Fig. 6. As can be observed, the sample mainly contains elongated nanoparticles with sizes smaller than 10 nanometers. On the other hand, the presence of aggregates of nanoparticles forming voids spaces or pores in the material is observed.

In general, when aluminum alkoxides are hydrolyzed with controlled amounts of water, two reactions can occur [19–22]:

$$Al(OR)_3 + 3H_2O \rightarrow Al(OH)_3 + 3ROH$$

$$Al(OR)_3 + 2H_2O \rightarrow AlOOH + 3ROH$$

As it can be observed, the amount of water added is critical, if three moles or more of water are added to one mole of aluminium isopropoxide, one mole of aluminium hydroxide is formed and three moles of isopropanol are liberated. Under the present experimental conditions, in water excess, different interactions may exist. These could be generated between the aluminum hydroxide surface and the resin acid, as the following reaction proceeds:

$$[Al(O)(OH)]_n \xrightarrow{HO_2CR} \left[Al(O)_x(OH)_y(O_2CR)_z\right]_n$$

The carboxylate ligand is covalently bound to the aluminum surface. The resulted material is known as carboxylate-alumoxane. The alumoxanes are chemically functionalized nanoparticles and may be selectively prepared with a particle size of 5–150 nm depending on the identity of the organic substituents and the processing conditions, this is removed only under extreme conditions [4–7]. In this way, three possible coordination modes of the carboxylate ligands and aluminum ions on the surface of boehmite may occur [4], among which the linkage to two Al atoms seems to be the most stable mode (Fig. 7). Thus, carboxylates get bonded to the surface of boehmite mostly via this mode. The reason for more stability of this mode of linkage is the formation of six-membered rings which are stabilized through resonance [4,23]. The reaction of boehmite with carboxylic acids is formed as consequence of the cleavage of the interlayer hydrogen bonds in the (1 0 0) plane of boehmite; the reaction of carboxylic acids with the double-layered aluminum oxide hydroxide (boehmite) may be ideally considered as an intercalation/exchange reaction where the acid replaces some of the hydroxyl groups on the oxide double layer surface and bridges other aluminum sites [17,24,25].

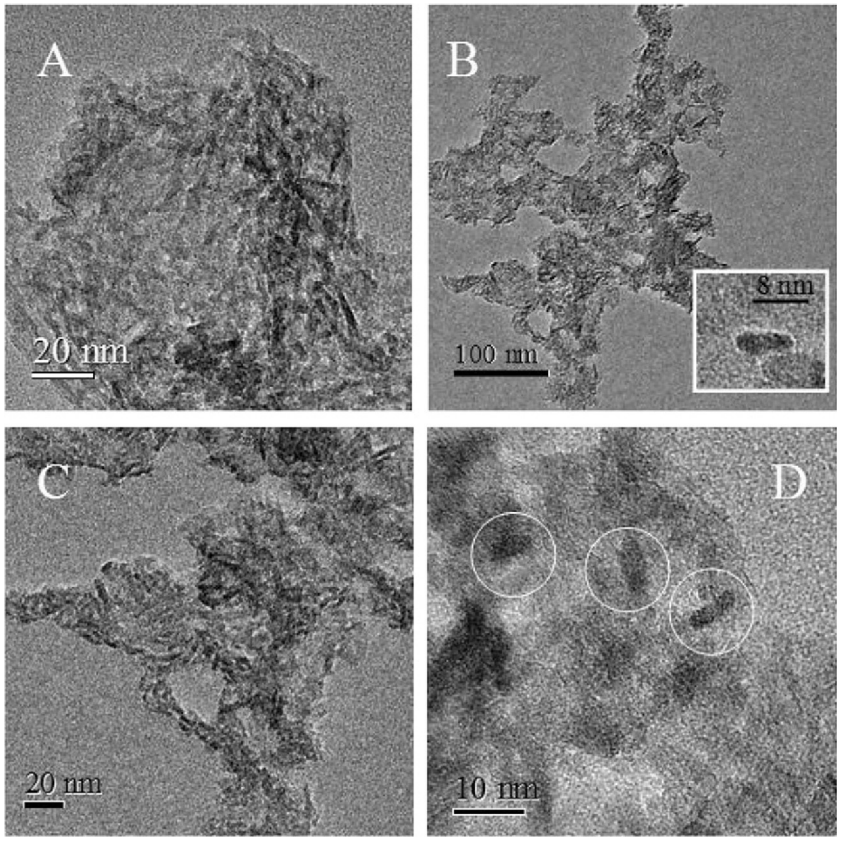

Fig. 6. HRTEM image of sample after calcination at 650 °C: (A) 100,000X, (B) 30,000X, (C) 60,000X, (D) 200,000X.

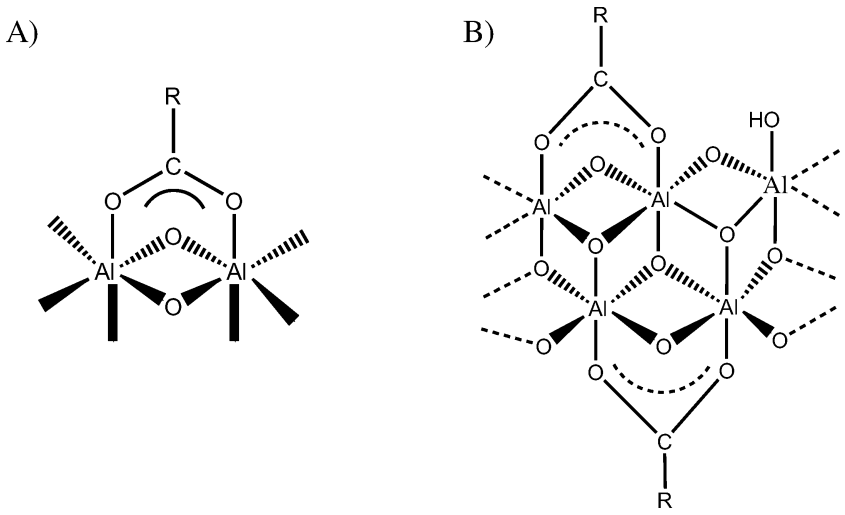

Fig. 7. Bridging mode of coordination of the carboxylate moiety to the boehmite core, (A) basic scheme and (B) 3D scheme.

The FTIR spectroscopy is a very useful method of characterization for these products. The carboxylate bonds show specific absorbing frequencies in the FTIR spectra.

A comparison of the FTIR spectra of the corresponding carboxylic acids used as precursors, the carboxylate alumoxanes and the alumina is shown in Fig. 8. The FTIR spectra (Fig. 8A) and the corresponding signal analysis presented in Table 1, shows the infrared absorption bands characteristics of the rosin employed (*Pinus Caribeae* from Venezuela). Included among them are: the region at 1500–1000 cm^{-1}, revealed the existence of several bands of different intensity which could be attributed to bonds type C═C and C—H [18,26]. The vibrations of the methyl groups appear at 1384 cm^{-1} and 1450–1411 cm^{-1} [27]. Characteristic absorption bands of isopropyl groups at 1150 cm^{-1} were observed. The presence of olefinics fragments (cyclic or exocyclic, *trans* or *cis*) was evident at 1083–1029 cm^{-1}. The existence of aromatic fragments was also observed close to 1500 and 1450 cm^{-1} [18,26,27].

A comparison of rosin spectrum with as-synthesized sample spectrum (Fig. 8B) revealed the presence of new absorption bands at 1636 and 1400 cm^{-1}, which could be assigned to the stretching vibrations produced by the bridging mode of coordination of the carboxylate groups that were bound to the boehmite core [3,20,21] (Fig. 2). This structure was proposed before for a product obtained from a reaction of boehmite with carboxylic acids [16], involving the heating of the reaction mixture for extended times. On the other hand, the IR spectra show a broad absorption band at 3700–3000 cm^{-1}, consistent with the assignment of aluminum-bound hydroxide groups. The weak band at 1073 cm^{-1} was attributed to the bending vibrations of the deprotonated hydroxyl groups [18,26]. These results confirmed that a carboxylate alumoxane was formed.

The FTIR spectrum of the calcined sample (Fig. 8C) is characterized by a broad band between 900 and 400 cm^{-1} attributed to stretching vibrations of Al—O bonds while the peak at 1470 cm^{-1} corresponds to Al═O bond stretching [3,20,21]. These results are consistent with the XRD analysis where the γ-phase was identified (Fig. 2). However, three signals are observed at 1636, 1515 and 1443 cm^{-1} which seemed to indicate that the alumina nanoparticles surface might be covered with covalently bound carboxylate groups (contain bridging carboxylates). This suggests that after calcination at a temperature of 650 °C remains carboxylate groups, which forms organic substituted alumina nanoparticles [17,24,25]. Additionally, it is important to mention that samples calcined at different temperatures (850–1000 °C) confirms the prevalence of these carboxylate groups.

It is known that the properties and processability of the carboxylate-alumoxanes are strongly dependent on the nature and size of the organic group attached to the boehmite core. It is expected that all the organic fraction was removed to obtaining only γ-alumina. However, the permanence of carboxylate groups at this temperature can be attributed to the complexity of the structures of rosin acids: partially unsaturated with one carboxyl group and three fused six-membered rings.

This organic substituted alumina ceramic nanoparticles could have interesting catalytic applications, could be doped at room temperature in aqueous solution with some metal cations to prepare novel catalyst and catalyst support materials. The ease of introduction of multiple cations into the alumina lattice via the alumoxane approach provides a method for fine-tuning catalyst support properties and the fabrication of new catalyst materials themselves [6,7]

Fig. 9(A and B) shows the N_2 physisorption isotherm and pore size distribution, respectively, of the calcined sample. The sample showed IV-type isotherm (definition by IUPAC) [26] which is characteristic of mesoporous material. The appearance of type H2 hysteresis loop in the isotherm indicates the presence of "ink-bottle" type pores [26]. The physisorption measurements revealed a large BET surface area (183 m^2/g), a pore volume of 0.4 $cm^3\,g^{-1}$), and a narrow pore size distribution, centred at ~10 nm pore diameter resulting from interparticulate voids existing between the nanoparticles (Fig. 9B).

3.1. Formation mechanism of porous structure

Pine resin contains compounds of low solubility in water. Among these, resin acids (Table 2) and fatty acids have been identified [28,29]. These hydrophobic components may exist as suspended colloids [30–34]. The reasons for this have been attributed to an increase in the stability of the colloidal droplets [30–34], due to changes in the surface charge density. These conditions would help the carboxylic acids groups on the hydrophobic molecules to become oriented towards the surface of the colloidal droplets. Moreover, the carboxylic acids groups would easily interact with the aluminum monohydroxide formed as a product of the hydrolysis of the aluminum alkoxide. Subsequently, this could allow the formation of a carboxylate alumoxane. In addition, it is known that these suspended colloids have an

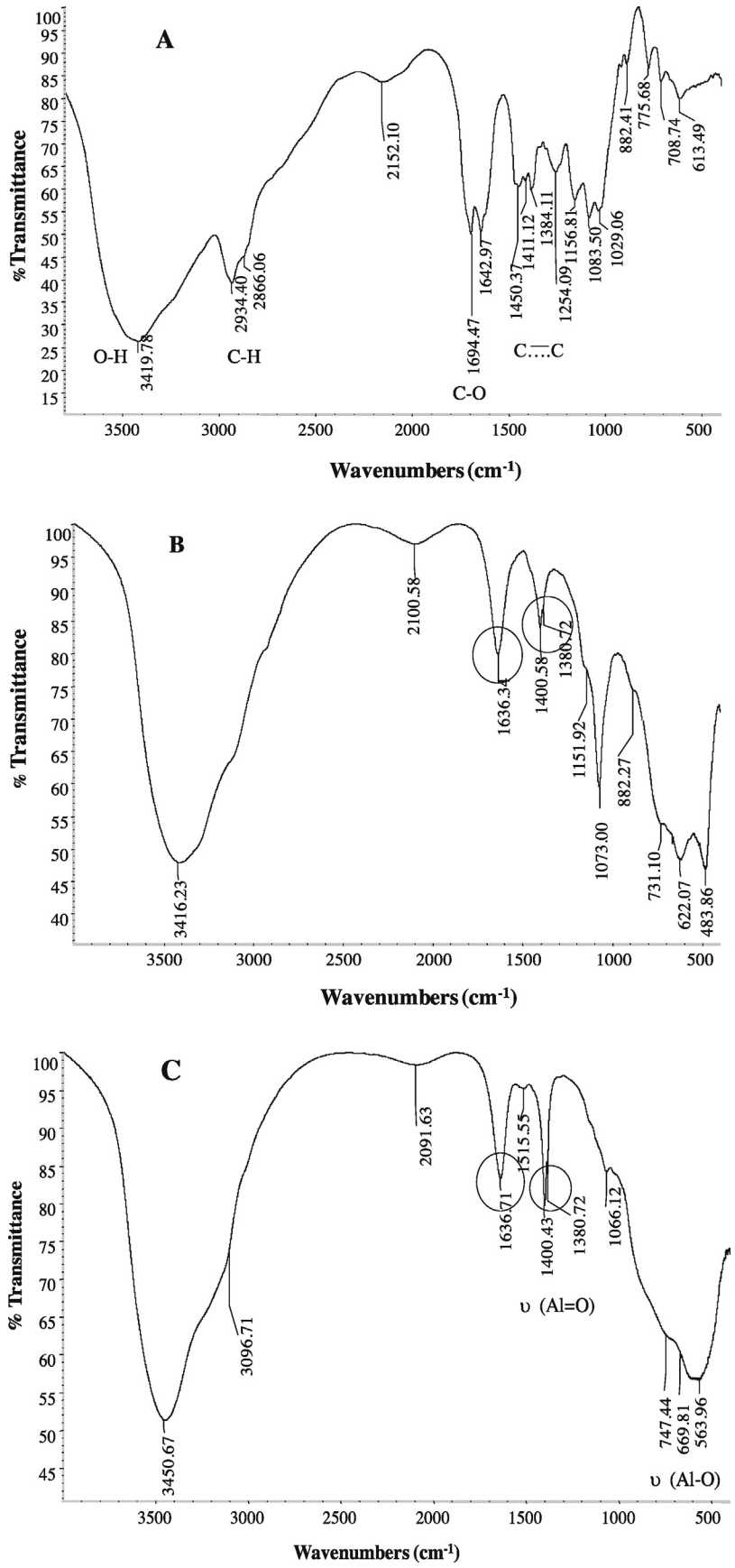

Fig. 8. FTIR spectra of (A) the pure rosin, (B) as-synthesized sample, and (C) the calcined sample.

Table 1
Infrared absorption bands characteristics of the rosin employed as template.

Characteristics absorption bands		Identification	Rosin family pinaceae	Rosin *Pinus Caribaea* Venezuela
Strong bands	2930–2958	C—H stretches	2936	2934
	1695–1715	Carbonyl bands, vinyl stretches and bends	1690–1700, 1697	1694
	2865–2875	C—H stretches	2870, 2646–2654	2866
Medium bands	1448–1467	Characteristic fingerprint region bands	1612	1643
	1382–1387		1496	1450
	1178–1184		1365	1384
	1078–1092		1275	
	1028–1032		1239	1254
	887–897		1151	1157
			1130	1084
			1107	1029
			980	
			910	882
			823	
			707	709
			652	614

Table 2
Solubility of resin acids in water, modified of Peng and Roberts [29].

Resin acid	Solubility (mg/L)
Dehydroabietic acid	5.1
Abietic acid	2.7
Levopimaric acid	2.5
Palustric acid	2.4

additional stability caused by the dissolved sugars from resin [31–38]. Among these have been mentioned, polysaccharides (galactoglucomannans, water soluble arabinogalactans) and monosacharides (xylose, glucose, galacturonic acid and galactose) [30–32].

After the reasons previously mentioned, it is considered that to determine the most prevalent components of *Pinus caribaea* rosin, a NMR study is required (Fig. 10).

In the ^{1}H NMR spectra corresponding to the mixtures of rosin acids used as template (Fig. 10), characteristic zones can be distinguished. The signals between 0.5–0.8 and 1.0–1.2 are attributed to the singlets and doublet of doublets generated by the presence of methyl groups [27,28]. The region between 1.3 and 2.0 ppm is a group of high multiplicity signals, associated with methylen groups. In the range 5.0–6.0 ppm it can be observed signals associated with the olefinic zone, endo and exocyclic bonds [27], which indicated the presence of the abietic acid. In addition, at 6.8–7.3 ppm there are four characteristic signals (3 aromatic protons) which may be associated to the dehydroabietic acid. The calculated spectra using ACD Labs package was in agreement with the experimental data (Fig. 10). To model the extract, it was proposed a theoretical mixture of resinic acids commonly found in the *Pinus caribaea* rosin. A comparison between the ^{1}H NMR experimental and calculated spectra revealed similar signal patterns. The study of both spectra allowed us to infer that the structure-directing agent consists of a mixture of resinic acids among which there are the abietic, dehydroabietic and levopimaric acids as major compounds. ^{13}C NMR spectrum (between 120 and 135 ppm) revealed the existence of a characteristic pattern of cyclic olefin, and aromatic systems. Moreover, at 179.6 ppm it was observed a signal confirming the existence of carboxylic functional group. Finally the typical area for signals corresponding to atoms of saturated carbon chains and cyclic subsystems (CH); (CH_2) is observed between 17 and 28 ppm [27]. The calculated ^{13}C NMR spectrum was consistent with that observed in ^{1}H NMR studies between 120 and 135 ppm.

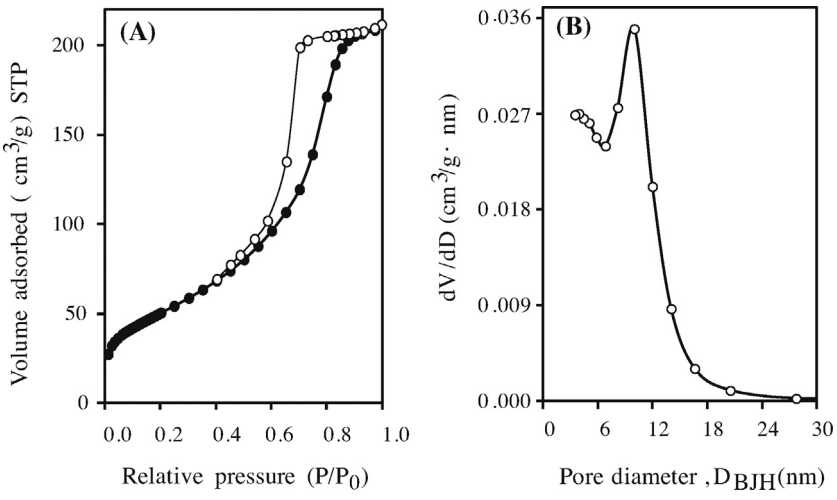

Fig. 9. Nitrogen adsorption–desorption isotherms of the calcined sample (A) and its pore size distribution calculated from the desorption branch (B).

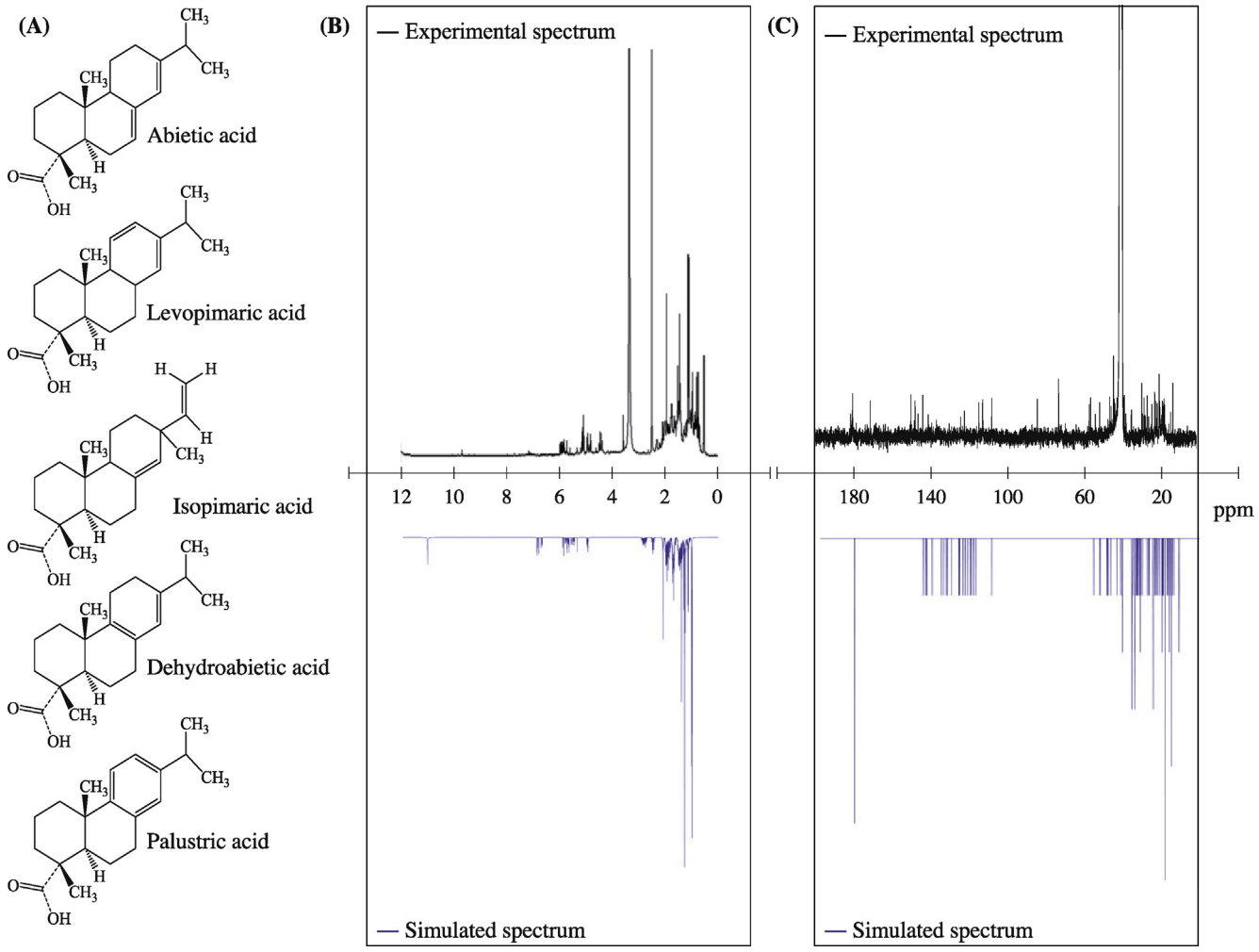

Fig. 10. ^{1}H NMR and ^{13}C NMR of experimental and calculated spectra for the mixtures of rosin acids.

4. Conclusions

We have shown that colophony extract obtained from *Pinus caribaea* can be used as a mixture of organic acids for preparation of carboxylate substituted Al_2O_3 nanoparticles. TEM micrographs show nanoparticles with range in size from 5 to 8 nm. The obtained materials displayed high surface areas (183 m^2/g) and narrow pore size distribution centred at 10 nm. FTIR analysis showed that carboxylate ligands are still bound to the aluminum oxide surface, even after calcination at 650 °C. The XRD patterns and ^{27}Al MAS NMR spectrum confirm the obtaining of γ-Al_2O_3 phase.

Acknowledgments

Financial support for this work was provided by the Instituto Venezolano de Investigaciones Científicas through Project 1077. To Lic. Liz Cubillán for assisting with the FTIR analyses. I am grateful to the editor and anonymous referees for helpful suggestions to improve this manuscript.

References

[1] A. Boumaza, L. Favaro, J. Lédion, G. Sattonnay, J.B. Brubach, P. Berthet, A.M. Huntz, P. Royc, R. Té Tot, Transition alumina phases induced by heat treatment of boehmite: an X-ray diffraction and infrared spectroscopy study, J. Solid State Chem. 182 (2009) 1171–1176.
[2] L.M. Perander, Z.D. Zujovic, M.M. Hyland, M.E. Smith, L.A. O'Dell, J.B. Metson, Short- and long-range order in smelter grade alumina–development of nano- and microstructures during the calcination of bayer gibbsite, light metals, Mineral Metals Mater. Soc. (2008) 29–35.
[3] C. Pecharroman, I. Sobrados, J.E. Iglesias, T. Gonzalez-Carreño, J. Sanz, Thermal evolution of transitional aluminas followed by NMR and IR spectroscopies, J. Phys. Chem. B 103 (1999) 6160–6170.
[4] A. Ashraf Derakhshan, L. Rajabi, H. Karimnezhad, Morphology and production mechanism of the functionalized carboxylate alumoxane micro and nano-structures, Powder Technol. 225 (2012) 156–166.
[5] R.L. Callender, C.J. Harlan, N.M. Shapiro, C.D. Jones, D.L. Callahan, M.R. Wiesner, D.B. Mac Queen, R. Cook, A.R. Barron, Aqueous synthesis of water-soluble alumoxanes: environmentally benign precursors to alumina and aluminum-based ceramics, Chem. Mater. 9 (1997) 2418–2433.
[6] A. Ashraf Derakhshan, L. Rajabi, Review on applications of carboxylate–alumoxane nanostructures, Powder Technol. 226 (2012) 117–129.
[7] W. Marsh, Chemical control over ceramic porosity using carboxylate-alumoxanes. European Patent Application, EP 1319 639 A2 (2003).
[8] E. Gerry, J.A. Hall, Biochemical phases of oleoresin production, Plant Physiol. 10 (1935) 537–543.
[9] S. Rezzi, A. Bighelli, V. Castola, J. Casanova, Composition and chemical variability of the oleoresin of *Pinus nigra* ssp. *laricio* from Corsica, Industrial Crop Prod. 21 (2005) 71–79.
[10] G.A. Smook, Handbook for pulp & paper technologists. Joint Textbook Committee of the Paper Industry, (1982).
[11] J.M. Gess, Rosin sizing of papermaking fibers, Tappi 72 (1989) 77–80.
[12] L.J. Stryker, E. Thomas Jr., B.D. Matijević, The formation of positively charged aluminum rosinate precipitates and their effect on paper sizing efficiency, J. Colloid Interface Sci. 43 (1973) 319–329.
[13] B.E. Yoldas, D.P. Partlow, Formation of continuous beta alumina film and coating at low temperatures, Am. Ceram. Soc. Bull. 59 (1980) 640–642.
[14] S. Brunauer, P.H. Emmett, E. Teller, Adsorption of gases in multimolecular layers, Amer. Chem. Soc. 60 (1938) 309–319.

[15] ACD/Labs Software, 133 Richmond St., W., Suite 605, Toronto, Ontario, Canada, M5H 2L5.
[16] A.A. Derakhshan, L. Rajabi, M. Marzban, Sh. Ghorabi, Synthesis and characterization of novel functionalized carboxylate-alumoxane nanostructures, Proceedings of the 4th International Conference on Nanostructures (ICNS4) Kish Island, I.R. Iran, 12–14 March, 2012).
[17] C.D. Jones, D.S. Brown, L.L. Marshall, A.R. Barrona, Carboxylate-Alumoxanes: Precursors for Heterogeneous Catalysts, MRS Proceedings 581, 659 (1999), doi: http://dx.doi.org/10.1557/PROC-581-659.
[18] L. Cook, L.S. DeVito, W. Myers, M. Smith, J. Elliott, C. Kreutzer, C. Wilson, M. Meiser, Nanoparticles modified with multiple organic acids, Patent No.:US 7244,498 B2, (2007).
[19] F. Vaudry, S. Khodabandeh, M.E. Davis, Synthesis of pure alumina mesoporous materials, Chem. Mater. 8 (1996) 1451–1464.
[20] A.B. Sifontes, G. Fragachán, J. Calderón, M. Mediavilla, R. Solano, J.L. Brito, L. Melo, Síntesis de óxidos de aluminio de alta área superficial y porosidad empleando un medio acuoso y carbohidratos como templates, CIENCIA 18 (2010) 65–75.
[21] Q.A. Liu Wang, X. Wang, T. Zhang, Mesoporous γ-alumina synthesized by hydro-carboxylic acid as structure-directing agent Micropor. Mesopor, Mat . 92 (2006) 10–21.
[22] K. B. Davison, Organic aluminium compounds. Patents United State 3184490.
[23] C.E. Bethley, C.L. Aitken, C.J. Harlan, Y. Koide, S.G. Bott, A.R. Barron, Structural characterization of dialkylaluminum carboxylates: models for carboxylate alumoxanes, Organometallics 16 (1997) 329–341.
[24] A. Kareiva, C.J. Harlan, D.B. Mac Queen, R.L. Cook, A.R. Barron, Carboxylate-substituted alumoxanes as processable precursors to transition metal-aluminum and lanthanide-aluminum mixed-metal oxides: atomic scale mixing via a new transmetalation reaction, Chem. Mater. 8 (1996) 2331–2340.
[25] M. Derrick, Fourier transform infrared spectral analysis of natural resins used in furniture finishe, JAIC 28 (1989) 43–56.
[26] J.L. Koenig, Application of FTIR spectroscopy to chemical systems, Appl. Spectrosc. 29 (1975) 193–309.
[27] R.M. Silverstein, F.X. Webster, D. Kiemle, Spectrometric Identification of Organic Compounds, seven ed., John Wiley Inc., New York, 2005.
[28] Y. He, Y. Zhang, J. Lu, R. Lin, Isolation and structural elucidation of abietic acid as the main adulterant in an herbal drug for the treatment of psoriasis, J. Pharmaceut. Bio-med. Anal. 66 (2012) 345–348.
[29] G. Peng, J.C. Roberts, Solubility and toxicity of resin acids, Water Res. 34 (2000) 2779–2785.
[30] J. Nylund, H. Byman-Fagerholm, J.B. Rosenholm, Physico-chemical characterization of colloidal material in mechanical pulp, Nord. Pulp Pap. Res. J. 8 (1993) 280–283.
[31] A.-L. Sihvonen, K. Sundberg, A. Sundberg, B. Holmbom, Stability and deposition tendency of colloidal wood resin, Nord. Pulp Pap. Res. J. 13 (1998) 64–67.
[32] H. Allen, Characterization of colloidal wood resin in newsprint pulps, Colloid Polym. Sci. 257 (1979) 533–538.
[33] A. Sundberg, K. Sundberg, C. Lillandt, B. Holmbom, Determination of hemicelluloses and pectins in wood and pulp fibres by acid methanolysis and gaschromatography, Nord. Pulp Pap. Res. J. 11 (1996) 216–219.
[34] K. Sundberg, C. Petterson, C. Eckerman, B. Holmbom, Preparation and properties of a model dispersion of colloidal wood resin from Norway spruce, J. Pulp Pap. Sci. 22 (1996) J248–J252J.
[35] K. Sundberg, J. Thornton, R. Ekman, B. Holmbom, Interactions between simple electrolytes and dissolved and colloidal substances in mechanical pulp, Nord. Pulp Pap. Res. J. 9 (1994) 125–128.
[36] I.A. Johnsen, M. Lenes, L. Magnusson, Stabilization of colloidal wood resin by dissolved material from TMP and DIP, Nord. Pulp Pap. Res. J. 19 (2004) 22–28.
[37] M. Chen, C.J. Biermann, Investigation of the mechanism of paper sizing through a desizing approach, Tappi J. 78 (1995) 120–126.
[38] S. Subrahmanyam, C.J. Biermann, Generalized rosin soap sizing with coordinating elements, Tappi J. 75 (1992) 223–228.